

We are IntechOpen, the world's leading publisher of Open Access books Built by scientists, for scientists

4,800

Open access books available

122,000

International authors and editors

135M

Downloads

Our authors are among the

154

Countries delivered to

TOP 1%

most cited scientists

12.2%

Contributors from top 500 universities



WEB OF SCIENCE™

Selection of our books indexed in the Book Citation Index
in Web of Science™ Core Collection (BKCI)

Interested in publishing with us?
Contact book.department@intechopen.com

Numbers displayed above are based on latest data collected.

For more information visit www.intechopen.com



Iron Oxide Nanoparticles Imaging Tracking by MR Advanced Techniques: Dual-Contrast Approaches

Shengyong Wu
Medical Imaging Institute of Tianjin
China

1. Introduction

Recently a number of imaging modalities have been presented for cellular imaging including magnetic resonance imaging (MRI), optical imaging, and positron emission tomography (PET) based on the background of growing demand for molecular imaging to noninvasively and longitudinally visualize cell migration and track transplanted cells *in vivo*, also to monitor cell biodistribution. Cellular MRI, with its superb ability of resolving soft tissue anatomies in three-dimensions (3D) with high spatial resolution in comparison to other modalities, is particularly important as a noninvasive tool to provide unique information on the dynamics of cell migration *in vivo* (Modo, 2005; Arbab, 2008a; Zhang, 2008).

In vivo MRI of cells is very useful for studying tumors, inflammation, stem cell therapy, and immune response, etc. Cells labeled with commercially available iron oxide nanoparticles (iron particles) can be imaged for weeks with MRI. The labeling procedure does not exhibit any alteration to cell viability or function (Bulte, 2004; Oude Engberink, 2007). Superparamagnetic iron oxides (SPIO) and ultra-small superparamagnetic iron oxide (USPIO) particles are commercial MR contrast agents for cell labeling due to their biocompatibility and strong effects upon T_2 and T_2^* relaxation. Several labeling methods have been developed to incorporate sufficient quantities of iron into cells. Cellular MRI has now been widely used for tracking transplanted iron-labeled therapeutic cells *in vivo* (Bulte, 2004; Oude Engberink, 2007). The technique has recently been introduced into the clinic (de Vries, 2005). The effect from iron particles is seen as hypointensity or negative-contrast on T_2 - and T_2^* -weighted images because of the shortening of T_2 and T_2^* relaxation times. However, concerns have been raised that the negative-contrast could be non-specific and difficult to differentiate from signal hypo-intensities resulting from susceptibility artifacts (i.e. from the presence of air or other field inhomogeneities), flow related signal losses, and calcification. Therefore, several positive-contrast and even dual-contrast imaging techniques have recently been developed for tracking iron-labeled cells. Dual-contrast imaging effectively permits detection of the presence of iron-labeled cells with both negative- and positive-contrast within a single image. This chapter illustrates negative- and positive-contrast MR techniques for tracking iron-labeled cells. Particular attention was paid to

recently developed positive-contrast cell tracking techniques, the status of dual-contrast approaches of new MRI pulse sequences and image postprocessing techniques and their perspectives. The new advanced technology in imaging contrast of iron oxide NPs on multimodal platform will also be introduced.

2. Negative-contrast MRI techniques

Cellular MRI is a newly emerging field of MR research that allows the “non-invasive, quantitative, and repetitive imaging of targeted macromolecules and biological processes in living organisms” (Herschman, 2003). Cellular MRI requires that cells are labeled with MR contrast agent to make them distinct from the surrounding tissues. Iron oxide nanoparticles are regarded as the most extensively applied contrast agent in cell imaging and cell tracking studies based on the fact of their strong negative contrast effect, biocompatibility, variety in core size and coating surface, as well as ease of detection at microscopic level (Muja, 2009). SPIO and USPIO are currently the predominant MRI contrast agents. The description of the physical and chemical properties of SPIO and USPIO can be found in recent reviews (Herschman, 2003; Thorek, 2006; Muja, 2009). The sizes of monocrystalline iron oxide nanoparticles (MIONs) ≈ 3 nm in diameter, USPIO particles ≈ 15 -30 nm, SPIO particles ≈ 60 -180 nm and micron sized iron oxide particles (MPIOs) can be as large as 10 μm (Shapiro, 2005). Some of the SPIO and USPIO agents, such as Endorem (SPIO, Guebert), Ferumoxides (SPIO, Berlex) and Resovist (USPIO, Schering), are already approved by the Food and Drug Administration (FDA) and are extensively used for imaging of the liver, central nervous system (CNS) and lymphatic system (Arbab, 2004b; Helmberger, 2005; Manninger, 2005), etc. Cationic transfection agents such as poly-L-lysine or the FDA-approved protamine sulfate are used to increase labeling efficiency *in vitro*. SPIO particles may decrease T_2^* by magnetic susceptibility effect and T_2 by dipole-dipole interaction or scalar effect between protons and magnetic centre. A large magnetisation difference occurs as a result of the nonhomogeneous distribution of superparamagnetic particles, which gives rise to local field gradients that accelerate the loss of phase coherence of the spins contributing to the MR signal. Iron-labeled cells cause significant signal dephasing due to the magnetic field inhomogeneity induced in water molecules near the cell such that iron-labeled cells were visualized as signal voids on T_2 and T_2^* weighted images (negative-contrast MR imaging). Negative-contrast techniques are the most commonly used approach for the detection of the SPIO-labeled cells.

While cell-based therapies have attracted well attention as novel therapeutics for the treatment of so many kinds of diseases, investigations (Zhang, 2005; Heyn, 2005, 2006) have showed that single, living, highly phagocytic large cells, such as macrophages, or human endothelial cells can be tracked over time in MRI using a 3.0 T even 1.5 T scanner. As an example of stem cell-based studies, investigators (Anderson, 2005) demonstrated that MRI of iron-labeled stem cells was directly identified in neovasculature of a glioma model. The cells were labeled using the ferumoxides/poly-L-lysine complex *in vitro* and the labeled cells were then injected in the model, and their migration toward and incorporation into the tumor neovasculature was visualized *in vivo* with negative-contrast MRI. Other studies have shown that ferumoxides-TA labeled human MSCs will home to liver (Arbab, 2004a), tumors (Khakoo, 2006), or heart (Kraitchman, 2005), illustrated at negative-contrast imaging with MR scan and confirmed at histologic evaluation. A group (Zhu, 2006) labeled neural

stem cells (NSCs) obtained from patients with traumatic brain injury then performed intracerebral injections of either ferumoxide-labeled or unlabeled cells around the injured tissue of them as the first study in the field of noninvasive imaging of stem cell treatment of brain injury, and their serial MRI about 7-10 weeks demonstrated that stem-cell engraftment and migration after implantation can be detected noninvasively with the use of MRI.

Also, in an early study (Kircher, 2003a), a highly derivatized cross-linked iron oxide (CLIO) nanoparticle was used to efficiently label cytotoxic T lymphocytes (CTLs) for in vivo tracking of the injected cells to melanoma cell line at near single-cell resolution, with MRI and optimized the labeling protocol (three-dimensional nature of the calculated T_2 maps), showing no cytotoxic and not influencing cell behavior or effector function. Despite the fact that the high spatial resolution given by MRI provides accurate evaluation of morphology of lymphoid organ, the sensitivity and ability to quantify MR data is still limited when compared with nuclear medicine based techniques. For MR cell tracking to be clinically useful, it should be defined for the detection limits of the MR method which will be utilized. The related clinical studies with 3.0 T scanners suggest that negative-contrast techniques possibly detect 150,000 Feridex labeled cells after directly injected into the lymph nodes of patients (de Vries, 2005). Another recent example of study by Laboratory for Gene Transcript Targeting, Imaging and Repair in Massachusetts General Hospital demonstrated that functionalization allows SPIO nanoparticles to be targeted, and it showed that their phosphorothioate-modified DNA probes linked to SPIO could be used to identify differential gene expression due to amphetamine exposure with high reliability using the calculation of rate of signal reduction (R_2^*) in T_2^* -weighted MR images (Liu, 2009). There are also extensive published works with detailed descriptions of many aspects of labeled cells for detection with negative-contrast MRI (Ferrucci, 1990; Bulte, 2004b; Hsiao, 2007; Gonzalez-Lare, 2009). Those and many of other preclinical studies have provided evidences for the potential translation of iron oxide NPs labeling and cellular MR imaging to the clinic applications.

An important property of USPIO is its ability to shorten T_1 and T_2 relaxation times (Small, 1993; Li, 2005). USPIO-labeled cells can be tracked in T_1 and T_2/T_2^* weighted images, which should increase the accuracy and the specificity for detection of the labeled cells (Kelloff, 2005), such as in imaging assessment on angiogenesis of tumor (Niu, 2011), atherosclerotic plaques (Metz, 2011), or arthritis (Lefevre, 2011). USPIO nanoparticles recently have shown potential in the imaging of molecular biomarkers, such as integrins that are heterodimeric transmembrane glycoproteins, a family of adhesion molecules playing a major role in angiogenesis and tumor metastasis (Chen, 2009; Tan, 2011).

Much of the progress in detecting individual iron-labeled cells has achieved from improvements in contrast agent design that increases targeting and intracellular uptake properties (Cerdan, 1989; Weissleder, 1990; Bulte, 2001; Zhao, 2002). Improvements in MR hardware and pulse sequence design also have played an important role during recent progress in this area of research. Although negative-contrast MRI has shown promise as a means to visualize labeled cells (Hogemann, 2003; Heyn, 2005), some remaining issues may hamper its wide applications: (1) it is difficult to distinguish the signal voids of labeled cells from those of complex background tissue signals; (2) With the resulting signal void as the means for detection, partial-volume effects are often severe and go far beyond the real cell

size; (3) it is difficult to discriminate iron-induced susceptibility changes from those caused by other susceptibility artifacts due to i.e. air/tissue interfaces, or peri-vascular effects.

3. Positive-contrast and dual-contrast MRI techniques

The “white-marker imaging” positive-contrast mechanism was introduced by Seppenwoolde et al. in 2003 (Seppenwoolde, 2003). Since then, several groups have developed positive-contrast or dual-contrast pulse sequences for tracking iron-labeled cells *in vitro* and *in vivo* (Table 1).

3.1 Gradient-dephasing technique: “white-marker” imaging

“White-marker” imaging was initially presented to create positive-contrast around paramagnetic intravascular device markers used in magnetic-resonance-based interventional procedures (Seppenwoolde, 2003). The gradient-dephasing technique uses a slice gradient to dephase the background water signal followed by an incomplete gradient rephasing pulse which was exploited for the depiction and tracking of paramagnetic susceptibility markers. Local magnetic field inhomogeneities were selectively visualized with positive-contrast, such as those created by iron-labeled cells for “white-marker” imaging. Advanced methods were developed to separate magnetic susceptibility effects from partial volume effects in “white marker” imaging in order to avoid compromising the identification of magnetic structures (Seppenwoolde, 2007). However, this method is only sensitive to macroscopic field inhomogeneities caused by paramagnetic material, to a volume surrounding the paramagnetic material that is free of other field variations (Zurkiya, 2006).

A similar gradient dephasing technique termed gradient echo acquisition for superparamagnetic particles (GRASP), by dephasing of the background signal, has been used to detect positive-contrast from superparamagnetic particles based on the phenomena that the z-rephasing gradient is reduced so that dipolar fields generated by the cells are rephased and positive signal can be observed (Mani, 2006a), also to image ferritin deposition in a rabbit model of carotid injury with relatively low concentrations of iron oxides at 1.5 T MR scanner (Mani, 2006b). The GRASP technique was used to successfully image low concentrations of ferumoxides (0.05 mM Fe corresponding to 2.8 μg Fe/mL) and ferritin (5 μg Fe/mL) in gel phantoms (Mani, 2006). GRASP “white-marker” imaging has several advantages including ease of implementation, high sensitivity, no influence on positive signal due to both B_0 and B_1 field inhomogeneities, and fast acquisition with various TE values. The feasibility of GRASP was tested to aid in dynamically tracking stem cells in a mouse model of myocardial infarction (Mani, 2008). Using T_2^* -GRE and GRASP techniques at 9.4 T scanner, iron-labeled embryonic stem cells were visualized in the border zone of infarcted mice at 24 hours, and 1 week following implantation. The positive signal in areas containing iron-loaded stem cells corresponded precisely with the signal loss detected within images produced with conventional GRE sequences. Regions that contained iron-labeled cells were confirmed by histology (Mani, 2008). The presence of the signal loss because of iron-labeled cells would have been difficult to detect on T_2^* -weighted images without using the positive-contrast sequence. The region of the myocardium containing the iron-labeled cells was clearly visible when both GRASP and T_2^* -weighted techniques (dual contrast imaging) were applied. Dual-contrast effects act to extend the signal change well beyond the location of the particle or

MR sequences	Contrast agents	Experimental conditions	Biological target	Application and Results
gradient-dephasing technique & GRASP	Ferritin	<i>In vitro</i> and <i>in vivo</i>	Endogeneous ferritin	Crush injured rabbit carotid arteries Myocardial infraction
	Ferumoxides	<i>In vitro</i> and <i>in vivo</i>	Embryonic stem cell-derived cardiac precursor cell	Injected into the hind limb of mouse
	Ferumoxides	<i>In vitro</i> and <i>in vivo</i>	Embryonic stem cell line TL-1	
off-resonance (OR) method	Ferumoxides	<i>In vitro</i> and <i>in vivo</i>	SPIO-luc-mouse embryonic stem cell	Injection into hindlimbs of mouse
Off-resonance saturation	mMION/ SPPM	Gel phantom/ <i>in vivo</i>	the $\nu\beta_3$ -expressing microvasculature	molecular imaging of cancer
IRON technique	MION-47	<i>In vivo</i>	Macrophage	Atherosclerotic plaque MR lymphography
	MION-47	<i>In vivo</i>	Macrophage	
SR-SPSP sequence	Ferumoxides	<i>In vitro</i> and <i>in vivo</i>	Human bone marrow stromal cells	Injection into the hind legs of mouse
FLAPS sequence	Ferumoxides	<i>In vitro</i> and <i>in vivo</i>	GFP-R3230Ac cell line	Injection into the hind legs of rat
UTE imaging	Ferumoxides	<i>In vitro</i> and <i>in vivo</i>	G6 glioma cells	Implanted cellular imaging
SWEET sequence	Ferumoxides	<i>in vivo</i>	Human epidermal carcinoma cells	Visualization of magnetically labeled tumor cells

Note: GRASP, superparamagnetic particles/susceptibility; IRON, oxide nanoparticles-resonant water suppression; SR-SPSP, self-refocused spatial-spectral; FLAPS, fast low-angle positive contrast steady-state free precession; UTE, ultrashort echo-time

Table 1. Summary of Previously Published Studies of Positive- and Dual-contrast Techniques

cell itself. This form of signal amplification increases sensitivity in detecting the labeled cells within a complex image background. With the use of signal amplification, potential future applications of (U)SPIO include 'doping' of therapeutic cell preparations with a small fraction of labeled cells, to allow cell tracking without altering the majority of the cells. This would allow for better delineation and identification of labeled cells with both techniques. The challenge for both techniques is the difficulty associated with attempting to quantify the concentration of the labeled cells *in vivo* because of the susceptibility artifact produced via the iron particles.

Generally, to resolve issues associated with volume averaging and other artifacts that may limit the clinical utility of MRI to detect iron labeled cells (especially in tissues other than the brain), GRASP technique has been developed to differentiate between the signal generated by the cells and signal loss caused by various artifacts (Mani, 2006, 2008), and to specifically avoid the signal loss generated by the iron laden cells to be confused with signal caused by other sources (motion, perivascular effects, coil inhomogeneities, etc.). In the recent study (Briley-Saebo, 2010), the GRASP sequence was also used to both detect and confirm the presence of the Feridex labeled dendritic cells (DCs) in the draining lymph nodes of nude mice 24 h after footpad injection. The results showed the possibility to detect and longitudinally track *ex vivo* human DC vaccines in the spleen of mice for up to 2 weeks, with greater lymphoid targeting observed following *i.v.* injection, relative to subcutaneous foot-pad injection; also showed good correlation between *in vivo* R_2^* values on a 9.47 Tesla dedicated mouse scanner and Feridex concentration, with detection limits of 3.2% observed for the spleen. But investigators didn't detect the Feridex labeled cells within the liver and spleen using the GRASP sequence while they indicated that, the dipole effects would be limited and signal enhancement would not be observed when the iron particles being homogeneously distributed over a large volume (such as the liver or spleen). They further demonstrated the values of nodes the white marker sequence, GRASP, in accurate detection and identification of Feridex labeled DCs in superficial lymph, and indicated that the appropriate utilization of animal models and MR validated imaging strategies might allow for the optimization of human DC vaccine therapies and improved therapeutic success, whereas white marker sequences may be most effective when the iron laden cells being compartmentalized within a limited volume (such as in lymph nodes, tumors, or myocardium). On the basis of a recent report (Sigovan, 2011) of the feasibility study on a positive contrast technique, GRASP at a relatively high field 4.7 T, for a novel superparamagnetic nanosystem designed for tumor treatment under MRI monitoring, investigators found that the magnetic nanoparticles for drug delivery can be detected using positive contrast, and suggested that the combined negative and susceptibility methods allow good quality images of large magnetic particles and offer their follow-up for theranostic applications.

3.2 Off-resonance Imaging (ORI)

Off-resonance MRI approaches have also been developed to produce positive-contrast. With this method, a spectrally selective radio frequency (SSRF) pulse was used to excite only the susceptibility-shifted, or 'off-resonance', water signals (Cunningham, 2005; Foltz, 2006), at the frequency shift induced by the iron particles. Since only the off-resonance signal due to

iron particles are excited and refocused, the background on-resonance signal is largely eliminated.

Iron-labeled mouse embryonic stem cells were imaged as positive-contrast through suppression of background tissue with these off-resonance methods (Suzuki, 2008). A spin-echo sequence was used with million-fold (120 dB) suppression of on-resonance water by matching the profiles of a 90° excitation and a 180° refocusing pulse. The positive-contrast signal from the volume of cells was affected by how well the excitation profile was defined. The method is therefore inherently limited by the complication associated with unwanted magnetization from the regions that suffer from chemical shift or susceptibility-related artifacts (e.g., from fat/lipid present in the region of interest and/or imperfect B_0 shimming, due to air/tissue interfaces, etc.) (Farrar, 2008). Although ORI techniques are being increasingly used to image iron oxide imaging agents such as MION, the diagnostic accuracy, linearity, and field dependence of ORI have not been fully characterized. After the sensitivity, specificity, and linearity of ORI were examined as a function of both MION concentration and magnetic field strength (4.7 and 14 T), and MION phantoms with and without an air interface as well as MION uptake in a mouse model of healing myocardial infarction were imaged, the linear relationship between MION-induced resonance shifts and with MION concentration were illustrated, whereas T_2 showed comparable to the TE and then decreasing after increasing initially with MION concentration and the ORI signal/sensitivity being highly non-linear. Improved specificity of ORI in distinguishing MION-induced resonance shifts and linearity can be expected at lower fields (4.7 T, on-resonance water linewidths 15 Hz) with on-resonance water linewidths decreased, air-induced resonance shifts reduced, and longer T_2 values observed, thus ORI will be likely optimized at low fields with very short TEs choosing and with moderate MION concentrations. Off-resonance approaches generate positive contrast but have a lower sensitivity than T_2^* -weighted imaging and are more complex to perform at high field strengths. Superparamagnetic iron-oxide nanoparticles become saturated above 0.5 Tesla and thus have equal sensitivity at clinical field strengths (1.5–3.0 T) and at the higher field strengths often used in preclinical studies (Sosnovik, 2009).

An alternative off-resonance technique termed inversion-recovery with on-resonant water suppression (IRON) sequence was proposed by a serial studies from one lab (Stuber, 2005, 2007). The IRON method used a spectrally-selective saturation pre-pulse to suppress the signal originating from on-resonant protons in the background tissue while preserving the signal from off-resonant spins in proximity to the iron particles. However, since the size of the signal-enhanced region is dependent on the bandwidth of the water suppression pulse, this scheme requires extra steps to adjust the center frequency and bandwidth of the pre-pulse to locate the exact site proximal to the cells. IRON sequence has been successfully applied for in vivo tracking of iron-loaded stem cells (Stuber, 2007).

The utility of IRON method combined with injection of the long-circulating MION-47 has been recently evaluated by investigators in Johns Hopkins University School of Medicine (Korosoglou, 2008a) for developing a novel contrast-enhanced MR angiography technique. One important aspect of the study was fat suppression for the IRON sequence with an initial radiofrequency pulse offset by 440 Hz at 3.0 T, and with spin inversion, to cause zero

longitudinal magnetization of the targeted species for the radiofrequency pulses (105° for fat, 100° for water), which obviously shortened the subsequent recovery time. The usage of MION-47 allowed acquisition of multiple image sets over a 1- or 2-day period with high spatial resolution.

IRON techniques with a commercially available MION-47 were recently employed to detect macrophage-rich atherosclerotic plaques in a rabbit model of atherosclerosis (Korosoglou, 2008b), in which pre-contrast imaging was performed in 7 Watanabe rabbits and 4 control New Zealand rabbits, and post-contrast imaging was repeated on days 1 and 3 after intravenous injection of MION-47. A second injection was performed on day 3 after imaging and post-contrast imaging performed again on day 6. There was a significant increase in signal intensity within aortic atherosclerotic plaques following administration of MION-47 (48% increase on day 3 and 72% increase on day 6) versus hypointensity (negative-contrast) in conventional MR images, but no enhancement was seen in control rabbits that lacked atherosclerosis. The positive-contrast regions corresponded to regions demonstrating deposition of iron particles within macrophage-rich atherosclerotic plaques. These findings not only validated that MION-47 is a successful imaging agent for macrophage-rich atherosclerosis, but also suggested that positive-contrast IRON MRI can be applied to the general class of iron oxide particles. This is significant as USPIO-enhanced MR imaging has been previously studied in human (Trivedi, 2006); enabling IRON MRI sequences to be directly applied to patient care.

Korosoglou et al. also investigated the utility of IRON techniques and MION-47 to create positive-contrast MR-lymphography (Korosoglou, 2008c). After six rabbits received a single bolus injection of 80 mmol Fe/kg MION-47, MRI was performed at baseline, 1 day, and 3 days using conventional T_1 - and T_2^* -weighted sequences and IRON. On T_2^* -weighted images, as expected, signal attenuation was observed in areas of para-aortic lymph nodes after MION-47 injection. However, using IRON the para-aortic lymph nodes exhibited very high contrast enhancement, which remained 3 days after injection. IRON in conjunction with iron particles can be therefore used to perform positive-contrast MR-lymphography, particularly 3 days after injection of the contrast agent, when signal is no longer visible within blood vessels. The proposed method may have the potential as an adjunct for nodal staging in cancer screening.

Iron-labeled radioembolization microspheres were visualized for in vivo tracking during trans-catheter delivery to VX2 liver tumors in a rabbit model (Gupta, 2008). The study was performed for real-time observation of microsphere delivery with dual-contrast techniques. The results showed significant changes in post-injection contrast-to-noise ratio (CNR) values from those of pre-injection at positions of microsphere deposition with both negative- and positive-contrast.

The off-resonance MRI method possesses some advantages including no need for dephasing gradients or saturation pulses, high suppression efficiency, and flexible selection of the excited frequency band to encompass spins in the vicinity of the iron particles without fat tissue off-resonance. This technique, however, was not slice-selective such that it can result in interference from insufficiently suppressed background signals or less background signal with regions of greater susceptibility excluded from the selected slice. This technique can also cause less on-resonant signal to be suppressed, has less flexibility in RF pulse design,

and can lead to less erroneous off-resonant signal detection in a multi-slice manner with individually shimmed slices (Zurkiya, 2006).

The off-resonance saturation method has been developed by Zurkiya and Hu, in which water protons are imaged with and without the presence of an off-resonance saturation pulse (Zurkiya, 2006). This method relies on diffusion-mediated saturation transfer to reduce the on-resonance MRI signal due to the off-resonance saturation (ORS) pulse, similar to chemical exchange saturation transfer techniques (Ward, 2000). This approach has been verified that greatly improved tumor detection accuracy over the conventional T_2^* -weighted methods because of its ability to turn "ON" the contrast of superparamagnetic polymeric micelles (SPPM) nanoparticles (Khemtong, 2009). SPPM nanoparticles encoded with cyclic (RGDfK) ligand (arginine-glycine-aspartic acid), cRGD, were able to target the $\alpha_v\beta_3$ -expressing microvasculature in A549 non-small cell lung tumor xenografts in mice. The results suggest that the combination of ORS imaging with cancer-targeted SPPM nanoparticles will show promise in detecting biochemical markers at early stages of non-small cell lung tumor development, and could further enhance the sensitivity of contrast and provide new opportunities in imaging biomarkers setting of *in vivo* tumor target.

The study (Zurkiya, 2008) transfected cells with genes from magnetotactic bacteria (i.e., MagA) under doxycycline-regulated gene expression, resulting in the intracellular production of iron oxide nanoparticles similar to synthetic SPION. MagA-expressing cells could be visualized by MRI after transplantation in the mouse brain after 5 d of induction with doxycycline. The generalized implementation of these techniques as treatment strategies in stem cell tracking needs to be explored. Investigators have recently inserted magnetic reporter genes into cells. After the expression of iron storage proteins formed stored iron then MRI can be used to detect it. Another transgene reporter, an adenoviral vector carrying a transgene for light- and heavy-chain ferritin protein to transfect cells has been shown that they could be detected by *in vivo* magnetic resonance imaging (Genove, 2005).

Balchandani et al. recently developed a self-refocused spatial-spectral (SR-SPSP) pulse, which is successful in creating positive-contrast images of SPIO-labeled cells (Balchandani, 2009). This pulse can enable slice-selective, spin-echo imaging of off-resonant spins without an increase in TE, which is essentially a phase-matched 90° SPSP pulse and a 180° SPSP pulse combined into one pulse. This results in a considerably shorter TE than possible with two separate pulses. The simultaneous spatial and spectral selectivity allows the imaging of off-resonant spins while selecting a single slice. The SR-SPSP pulse is also suitable for any application requiring spatial and spectral selectivity, such as tracking metallic devices or replacing standard pulses in MR spectroscopic imaging sequences. More recently a novel combination of off-resonance (ORI) positive-contrast MRI and T_{2p} relaxation in the rotating frame (ORI- T_{2p} method) for positive-contrast MR imaging of USPIO in a mouse model of burn trauma and infection with *Pseudomonas aeruginosa* (PA), was also reported to have direct implications in the longitudinal noninvasive monitoring of infection, and show promise in testing the new-developed anti-infective compounds (Andronesi, 2010). The same group also reported that ORI- T_{2p} method proved to have slightly higher sensitivity than ORI, and MR imaging clearly showed migration and accumulation of labeled MSCs to the burn area which can be confirmed by histology staining for iron labeled cells (Righi, 2010).

3.3 Fast low angle steady-state free precession (FLAPS) sequence

FLAPS imaging has been proposed for time-efficient acquisition of off-resonance positive-contrast images (Dharmakumar, 2007). The technique takes advantage of the unique spectral response of the steady-state free precession (SSFP) signal to achieve signal enhancement from off-resonant spins while suppressing signal from on-resonant spins at relatively small flip angles (Dharmakumar, 2006). Besides the positive-contrast generated by the weakly off-resonant spins, the spins in and around the core of the local magnetic susceptibility (LMS)-shifting media (such as labeled cells) experience large deviations from the central frequency leading to intra-voxel dephasing that was observed as negative-contrast in FLAPS images. So this technique has the capability to identify the presence of labeled cells with both negative- and positive-contrast within a single image.

Zhang et al. recently investigated the feasibility of imaging iron-labeled green fluorescent protein (GFP)-expressing cells with the dual-contrast method and compared its measurements with traditional negative-contrast technique (Zhang, 2009). The GFP-cell was incubated for 24 hours using 20 mg Fe/mL concentration of SPIO and USPIO nanoparticles. The labeled cells were imaged using the FLAPS technique, and FLAPS images with positive-contrast were compared with negative-contrast T_2^* -weighted images. The results demonstrated that SPIO and USPIO labeling of GFP cells had no effect on cell function or GFP expression, and the labeled cells were observed as a narrow band of signal enhancement surrounding signal voids in FLAPS images. Positive- and negative-contrast images were both valuable for visualizing labeled GFP-cells. MRI of labeled cells with GFP expression holds great potential for monitoring the temporal and spatial migration of gene markers and cells, and enhances our understanding of cell- and gene-based therapeutic strategies. These findings suggested that the dual-contrast nature of the FLAPS approach offers significant advantages to the field of cellular MRI. A highly sought feature of cellular imaging is the quantification of labeled cells. Past studies have shown that it may be possible to define a relation between number of cells and MR transverse relaxation time constants (apparent T_2 or T_2^*). However, since the specificity of the labeled cells is often compromised in GRE images, it is often difficult to use the time constant thus derived as a reliable metric to quantify the number of cells. These previous FLAPS investigations showed that local contrast was exponentially related to the number of cells. Furthermore, the dual-contrast filter, using an image metric that is analogous to local contrast, can provide additional quantitative information regarding those regions containing the labeled cells. This technique still could be limited by the magnetic perturbations around MNPs. A careful investigation of how the output of dual-contrast image filters can be used to derive quantitative information regarding the concentration of labeled cells from *in vivo* images has been demonstrated (Dharmakumar, 2009).

3.4 Ultra short echo time methods

It has been introduced that ultrashort echo-time (UTE) imaging had capability of imaging materials with extremely short T_2 and very fast signal decay (Robson, 2006; Rahmer, 2009), and did as a new and promising approach that allowed the detection of short- T_2 signal components, such as tendons, ligaments, menisci, periosteum, and cortical bone before signals within these tissues decay to a level where they were not observable with conventional spin echo pulse sequences. Due to the very short TE (on the order of 1/10 ms)

used for UTE imaging, only negligible T_2 decay occurs before sampling, and consequently high signal from the short- T_2 components can be obtained. Coolen et al. reported that MRI parameters could be optimized for positive-contrast detection of iron-oxide labeled cells using double-echo Ultra-short echo time (d-UTE) sequences (Coolen, 2007). During these studies, there was a linear correlation between signal intensity and concentration USPIO labeled cells. Another group found that the enhancement due to the presence of short T_2 USPIO accumulation generally agreed with signal loss within GRE images during ex vivo MR of aorta atherosclerotic rabbit (Crowe, 2005).

Liu et al. recently measured ultrashort T_2^* relaxation in tissues containing a focal area of SPIO nanoparticle-labeled cells. MRI experiments in phantoms and rats with iron-labeled tumors demonstrated that these cells can be detected even at ultrashort T_2^* down to 1 ms or less (Liu, 2009). The authors suggested that combining ultrashort T_2^* relaxometry with the multiple gradient echo T_2^* mapping techniques should improve the ability to measure the relaxation of tissues with high densities of implanted iron-labeled cells. In another investigation, T1-weighted positive contrast enhancement from SPIO particles was achieved from the UTE imaging then this sequence, taking advantage of the unique effect of MNPs on relaxation time domain, was also examined to validate its positive contrast imaging capability of "probe" targeting to U87MG human glioblastoma cells through an SPIO conjugated RDG with high affinity to the cells overexpressing integrin $\alpha_v\beta_3$ (Zhang, 2011). So the study was regarded as providing a dual contrast imaging method from UTE technique plus T_2 -weighted TSE images in its application of molecular imaging of glioma with potential quantification of SPIO nanoparticles suggested by previously published report (Liu, 2009).

The more recent study (Girard, 2011) showed that both contrast mechanisms of optimizing T_1 contrast from UTE technique with conventional T_2^* contrast of SPIO, even an extra subtraction of a later echo signal from the UTE signal, could be powerful both in improving the specificity by providing long T_2^* background suppression and increasing detection sensitivity, in molecular imaging application of tumor-targeted IONPs in vivo. A hybrid sequence, PETRA (Pointwise Encoding Time reduction with Radial Acquisition) (Grodzki, 2011), combined the features of single point imaging with radial projection imaging with no need of hardware changes, to show shorter encoding times over the whole k-space and to enable higher resolution for tissue with very short T_2 , compared to the UTE sequence, so that it could avoid problems derived from the UTE but with good image quality and might improve e.g. orthopedic MR imaging as well as MR-PET attenuation correction. A 3D imaging technique (Seevinck, 2011) from the group in University Medical Center Utrecht, The Netherlands, applying center-out Radial Sampling with Off-Resonance reception (co-RASOR) by the using of UTE technique (for the minimization of subvoxel dephasing at locations with high magnetic field gradients in the vicinity of the magnetized objects), and a hard, nonselective RF block pulse and radial sampling of k-space, was also presented to depict and accurately localize small paramagnetic objects with high positive contrast but ideally without background signal.

3.5 Others new MRI pulse sequences and image postprocessing techniques

Several other new sequences were reported on positive- and dual-contrast methods of MR cell tracking. Kim et al. recently developed simple means of detecting iron-labeled cells by

using susceptibility weighted echo-time encoding technique (SWEET) (Kim, 2006). The subtraction of two sets of image volumes acquired at slightly-shifted echo time generates positive-contrast at the cell position. In a more recent study, the SWEET method was employed to selectively enhance the effect of the magnetic susceptibility caused by SPIO-labeled KB cells (KB cell is a cell line derived from a human carcinoma of the nasopharynx, used as an assay for antineoplastic agent). It was also demonstrated that this method could be used to visualize SPIO-labeled KB cells and their tumor formation in mice for at least a 2-week period (Kim, 2009).

Dual-contrast images can also be achieved by applying T_2^* -weighted imaging combined with different post-processing techniques from the magnetic field map (Ward, 2000; Zurkiya, 2006). A susceptibility gradient mapping (SGM) technique has been recently developed, in which a color map of 3D susceptibility-gradient vector for every voxel is generated with calculated echo-shifts, and the map presents a 3D form of a positive-contrast images (Dahnke, 2008; Liu, 2008). Hyperintensities of SGM were seen in areas surrounding the 1×10^6 ferumoxides/protamine sulfate complex labeled flank C6 glioma cells of experimental rat model. The sensitivity of the method was compared to white-marker and IRON positive-contrast methods for visualizing the proliferation of tumor cells for labeled tumors that were approximately 5mm (small), 10 mm (medium) and 20 mm (large) in diameter along the largest dimension (Liu, 2008). The number of positive voxels detected around small and medium tumors was significantly greater with the SGM technique than those with the other two techniques, while similar as the “white-marker” technique for large tumors that could not be visualized with the IRON technique. The SGM is a post-processing technique and its positive-contrast images can be derived directly from the T_2^* -weighted images without requiring dedicated positive-contrast pulse sequences, thereby it can provide the flexibility to display susceptibility gradients or suppress susceptibility artifacts in specific directions; not like the “white marker” or IRON techniques that require specialized pulse sequence designs and extra scans in addition to those obtained for conventional anatomic imaging. With SGM the hyperintense regions on positive-contrast images originating from SPIO labeled cells can be easily differentiated from other signal voids in T_2 or T_2^* -weighted images.

The phase gradient mapping (PGM) techniques have recently developed independently by two groups, one related derived phase gradient maps from standard phase images also including a phase unwrapping procedure to assist the analysis and characterization of object-induced macroscopic phase perturbations (Bakker, 2008); another one utilized fast Fourier transform (FFT) to form phase gradients and develop positive contrast maps by the use of PGM but without need of phase unwrapping, so as to be appropriate technique for the visualization of magnetic nanoparticulate system (Langley, 2011; Zhao, 2011). By the method introduced recently of dual contrast with therapeutic iron nanoparticles at 4.7 T scanner (Sigovan, 2011), or postprocessing methods, with the measure of the T_2^* , an efficient estimation of nanoparticle concentration can be made (Langley, 2011). Applications of two kind of approaches, the traditional relaxometry method and model-based method, have demonstrated that, besides the detection of SPIO nanoparticles by positive contrast methods, quantification of the SPIO concentration also play important role in clinical evaluation of results from different treatments with monitoring cellular therapies, and the

former derives from the signal decay associated with areas containing contrast SPIO particles (Kuhlper, 2007; Rad, 2007; Liu, 2009), assuming that the rate varies linearly with contrast agent concentration; the later derives from the formation of magnetic field by SPIO-containing region (Dixon, 2009).

3.6 T_1 & T_2 (T_2^*) multi-contrast for cell tracking

As introduced in as earlier as 1990s, it is possible to achieve positive contrast and dual contrast with superparamagnetic particles by employing T_1 - and/or T_2 -weighted sequences (Canet, 1993; Chambon, 1993; Small, 1993). Although most earlier clinical trials with magnetic nanoparticles as contrast agents were evaluated almost exclusively on T_2 -w fast spin echo (FSE) and T_2^* -w gradient echo (GRE) sequences, and the strong T_1 contrast enhancement effect of magnetic nanoparticles has rarely been used in clinical and molecular imaging (Reimer, 1995; Yamamoto, 1995; Tang, 1999), the effect of SPIO or USPIO on proton relaxation is not confined to T_2 and T_2^* effect. They should be considered to influence T_1 relaxivity with increased SI on T_1 -w GRE sequences at low concentrations. For *in vivo* imaging application of MNPs, optimal combination of negative and positive contrast methods is still under evaluation.

Superparamagnetic iron oxide particles (SPIO) were used shortly after gadolinium-chelate magnetic resonance (MR) contrast agent as well known, while USPIO being the strong T_2 relaxivity that produces negative contrast also a high T_1 relaxivity with an increase in SI on T_1 -weighted images (Small, 1993), so that a biphasic imaging sequence protocol (only immediate postadministration and 20-24 hr delayed images) in the *in vivo* study allowed visualization of the dynamic enhancement patterns of both normal tissue and potentially tumor based on early T_1 -shortening effects produced by intravascular USPIO particulate agent (BMS 180549, previously AMI-227) and marked T_1 -shortening produced following agent uptake by liver and spleen, as well as showed markedly less T_2 -shortening at 20-24 hr within both liver and spleen.

The more recent investigation (Zhang, 2011) demonstrated that an appropriate SPIO core size and concentration range was paid much attention to obtain positive contrast with UTE imaging, and this technique could be used with the receptor targeted SPIO molecular imaging probe so as to provide an opportunity for monitoring cancer cells with overexpression of integrin $\alpha_v\beta_3$ in addition to negative contrast by the approach of T_2 relaxometry mapping.

Investigators recently synthesized a biocompatible water-dispersible $\text{Fe}_3\text{O}_4\text{-SiO}_2\text{-Gd-DTPA-RGD}$ nanoparticle with r_1 relaxivity of $4.2 \text{ mm}^{-1}\text{s}^{-1}$ and r_2 relaxivity of $17.4 \text{ mm}^{-1}\text{s}^{-1}$ at the Gd/Fe molar ratio of 0.3:1, indicating the potential to use this multifunctional agent for dual-contrast MR imaging of tumor cells over-expressing high-affinity $\alpha_v\beta_3$ integrin *in vitro* and *in vivo* (Yang, 2011).

4. Imaging contrast of IRON-labeled cell on multimodular platform

MRI can be commonly used to set up a kind of nanomedicine platform for applications of multimodality probe to obtain information about concomitant anatomic, chemical, and physiological features of body. This kind of approach has been found under the

background that, the nanomedicine platform could capitalize on the availability of specific probes, while achieving an theranostic (integrated diagnostic and therapeutic) design to allow for the visualization of therapeutic efficacy by noninvasive imaging methods such as MRI (Guthi, 2010), for example, in the field of tumor imaging researches, the combination of diagnostic capability with therapeutic intervention is critical to address the challenges of cancer heterogeneity and adaptive resistance, also molecular diagnosis by imaging is important to verify the cancer biomarkers in the tumor tissue and to guide target-specific therapy. It has been thought that ideal multimodality imaging probes enhance capabilities from complementary imaging modalities to enable both noninvasive and invasive molecular imaging (e.g. via probes with MRI and NIR fluorescence reporter capabilities) and to facilitate verification of disease detection and deliver additional evidences for the pathology (eg, probes with reporter capabilities for both positron emission tomography and MRI) (Kircher, 2003b; Lee, 2008). As for the establishment and utilizations of multimodular platform, such as optical and multimodality molecular imaging; multifunctional PET/MRI contrast agent; focused ultrasound/magnetic nanoparticle targeting delivery; design magnetic nanoparticles, etc, some topics are beyond of the scope of this chapter, and some good review papers have already published, so readers are recommended to check them (Jaffer, 2009; Chomoucka, 2010; Liu, 2010; Veiseh, 2010).

Guthi et al. recently introduced a multifunctional methoxy-terminated PEG-b-PDLLA micelle system that was encoded with a lung cancer-targeting peptide (LCP) and loaded with SPIO together with doxorubicin for MR imaging and therapeutic delivery in their *in vitro* study of a lung cancer (Guthi, 2010), they presented a significantly increased cell targeting, micelle uptake, superb T_2 relaxivity for ultrasensitive MR detection and cell cytotoxicity in $\alpha_v\beta_6$ -expressing lung cancer cells, with confocal laser scanning microscopy of Doxo fluorescence also used to study the targeting specificity of LCP-encoded micelles to $\alpha_v\beta_6$ -expressing H2009 over the $\alpha_v\beta_6$ -negative H460 cells. The same micelles were previously conjugated with a cRGD ligand that can target $\alpha_v\beta_3$ integrins on tumor endothelial (SLK) cells (Nasongkla, 2006), illustrating growth inhibition of tumor SLK cells with ultrasensitive detection by MRI. The same lab in University of Texas Southwestern Medical Center at Dallas has previously demonstrated a multi-functional micelle design that allows for the vascular targeting of tumor endothelial cells, MRI ultrasensitivity, and controlled release of doxorubicin (Doxo) for therapeutic drug delivery (Nasongkla, 2006; Khemtong, 2009). Investigators (Guthi, 2010) found that SPIO-clustered polymeric micelle design has considerably decreased the MR detection limit to subnanomolar concentrations ($< \text{nM}$) of micelles through the increased T_2 relaxivity and high loading of SPIO per micelle particle; suggested that, on that multifunctional platform, the application of positive contrast imaging, such as ORS, could further enhance the contrast sensitivity and allow for the *in vivo* imaging of tumor-specific markers.

The proposed approaches of dual imaging (e.g. with CLIO modified with a NIR fluorophore, therapeutic siRNA sequences, and a cell penetrating peptide for cancer) (Medarova, 2007), even multi-modular imaging (e.g. with triple functional iron oxide nanoparticles) (Xie, 2010) demonstrate potential for the creation of targeted multifunctional nanomedicine platforms.

5. Perspectives

There is an increasing interest in using cellular MRI to monitor behavior and physiologic functions of iron-labeled cells in vivo. Iron particles provide good MR probing capabilities and some of these agents are currently available for clinical applications. Based on the fact that iron particles exhibit unique nanoscale properties of super-paramagnetism and have the potential to be utilized as excellent probes for cellular imaging and molecular imaging, several MR techniques have recently been proposed to increase the detection sensitivity for image contrast generated with iron-labeled cells, including negative-, positive- and dual-contrast methods for visualization of iron-labeled cells in vitro and in vivo.

The hyperintense regions on positive-contrast images originating from iron-labeled cells can be easily differentiated from other signal voids on T_2 or T_2^* -weighted images, therefore providing a greater degree of certainty in the determination of labeled cells. Moreover, the hyperintensities appeared to illustrate a greater sensitivity than the dark spots on regular MR images. Because positive-contrast imaging approaches do not provide sufficient anatomical information, it is necessary to combine positive-contrast techniques with conventional gradient echo or spin echo imaging, to achieve dual-contrast. Also, the combined gadolinium and SPIO-enhanced imaging in a 'dual contrast' MRI could be the more accurate technique for the detection of entities, especially of tumors. Additionally, some new applications of agents for MR imaging have been tested so as to obtain dual-contrast agents for noninvasive imaging studies. Dual-contrast MRI techniques for in vivo cell tracking will add to the growing armamentarium for preclinical cellular MR imaging and further demonstrate the value and diagnostic power of molecular MR imaging, and multifunctional iron oxide nanoparticles together with MRI will have unique advantages with diagnostic and therapeutic capabilities. Simultaneously, the "concept" of dual-contrast imaging can be expanded into imaging evaluation on the platform of dual-modality (or even multimodal approach) including the simultaneous MRI-PET of new method for functional and morphological imaging with blooming perspectives for further development.

While much progress has been made to date, many challenges still face cellular MRI approaches aimed at assessing the migration, homing and function of transplanted therapeutic iron-labeled cells in vivo. For cellular MRI techniques to be successful, the combined expertise of basic scientists, clinicians and representatives from industry will undoubtedly be essential.

6. References

- Anderson, S., Glod, J., Arbab, A., Noel, M., Ashari, P., Fine, H., & Frank, J. (2005). Noninvasive MR Imaging of Magnetically Labeled Stem Cells to Directly Identify Neovasculature in a Glioma Model. *Blood*, Vol. 105, No. 1, (August 2004), pp. 420-425, ISSN 0006-4971
- Andronesi, O., Mintzopoulos, D., Righi, V., Psychogios, N., Kesarwani, M., He, J., Yasuhara, S., Dai, G., Rahme, L., & Tzika, A. (2010). Combined Off-resonance Imaging and T_2 Relaxation in The Rotating Frame for Positive Contrast MR Imaging of Infection in a Murine Burn Model. *J Magn Reson Imaging*, Vol. 32, No. 5, (November 2010), pp. 1172-1183, ISSN 1053-1807

- Arbab, A., Jordan, E., Wilson, L., Yocum, G., Lewis, B., & Frank, J. (2004a). In Vivo Trafficking and Targeted Delivery of Magnetically Labeled Stem Cells. *Hum Gene Ther*, Vol.15, No. 4, (July 2004), pp. 351-360, ISSN 1043-0342
- Arbab, A., Yocum, G., Kalish, H., Jordan, E., Anderson, S., Khakoo, A., Read, E., & Frank, J. (2004b). Efficient Magnetic Cell Labeling with Protamine Sulfate Complexed to Ferumoxides for Cellular MRI. *Blood*, Vol. 104, No. 4, (April 2004), pp. 1217-1223, ISSN 1053-1807
- Arbab, A., & Frank, J. (2008). Cellular MRI and Its Role in Stem Cell Therapy. *Regen Med*, Vol. 3, No. 2, (March 2008), pp. 199-215, ISSN 1746-0751
- Bakker, C., de Leeuw, H., Vincken, K., Vonken, E., & Hendrikse, J. (2008). Phase Gradient Mapping as an Aid in The Analysis of Object-induced and System-related Phase Perturbations in MRI. *Phys. Med. Biol.*, Vol. 53, No. 18, (September 2008), pp. N349-N358, ISSN 0031-9155
- Balchandani, P., Yamada, M., Pauly, J., Yang, P., & Spielman, D. (2009). Self-refocused Spatial-spectral Pulse for Positive Contrast Imaging of Cells Labeled with SPIO Nanoparticles. *Magn Reson Med*, Vol. 62, No. 1, (May 2009), pp. 183-192, ISSN 0740-3194
- Briley-Saebo, K., Leboeuf, M., Dickson, S., Mani, V., Fayad, Z., Palucka, A., Banchereau, J., & Merad, M. (2010). Longitudinal Tracking of Human Dendritic Cells in Murine Models Using Magnetic Resonance Imaging. *Magn Reson Med*, Vol. 64, No. 5, (October 2010), pp. 1510-1519, ISSN 0740-3194
- Bulte, J., Trevor Douglas, T., Witwer, B., Zhang, S., Strable, E., Lewis, B., Zywicke, H., Miller, B., van Gelderen, P., Moskowitz, B., Duncan, I., & Frank, J. (2001). Magnetodendrimers Allow Endosomal Magnetic Labeling and In Vivo Tracking of Stem Cells. *Nature Biotechnology*, Vol. 19, No. 12, (December 2001), pp. 1141-1147, ISSN 1087-0156
- Bulte, J., & Kraitchman, D. (2004a). Iron Oxide MR Contrast Agents for Molecular and Cellular Imaging. *NMR Biomed*, Vol. 17, No. 7, (November 2004), pp. 484-499, ISSN 0952-3480
- Bulte, J., & Kraitchman, D. (2004b). Monitoring Cell Therapy Using Iron Oxide MR Contrast Agent. *Curr Pharm Biotechnol*, Vol. 5, No. 6, (December 2004), pp. 567-584, ISSN 1389-2010
- Canet, E., Revel, D., Forrat, R., Baldy-Porcher, C., de Lorgeril, M., Sebbag, L., Vallee, J., Didier, D., & Amiel, M. (1993). Superparamagnetic Iron Oxide Particles and Positive Enhancement for Myocardial Perfusion Studies Assessed by Subsecond T1-weighted MRI. *Magn Reson Imaging*, Vol. 11, No. 8, (March 2004), pp. 1139-1145, 0730-725X
- Cerdan S, Lötscher HR, Künnecke B, Seelig J. (1989). Monoclonal Antibodycoated Magnetite Particles as Contrast Agents in Magnetic Resonance Imaging of Tumors. *Magn Reson Med*, Vol. 12, No. 2, (November 2005), pp. 151-163, ISSN 0740-3194
- Chambon, C., Clement, O., Blanche, R., Schouman-Claeys, E., & Frija, G. (1993). Superparamagnetic Iron Oxides as Positive MR Contrast Agents: In Vitro and In Vivo Evidence. *Magn Reson Imaging*, Vol. 11, No. 4, (March 2004), pp. 509-519, ISSN 0730-725X
- Chen, K., Xie, J., Xu, H., Behera, D., Michalski, M., Biswal, S., Wang, A., & Chen, X. (2009). Triblock Copolymer Coated Iron Oxide Nanoparticle Conjugate for Tumor Integrin

- Targeting. *Biomaterials*, Vol. 30, No. 36, (September 2009), pp. 6912–6919, ISSN 0142-9612
- Chomoucka, J., Drbohlavova, J., Huska, D., Adam, V., Kizek, R., & Hubalek, J. (2010). Magnetic Nanoparticles and Targeted Drug Delivering. *Pharmacol Res*, Vol. 62, No. 2, (February 2010), pp. 144-149, ISSN 1043-6618
- Coolen, B., Lee, P., Shuter, B., & Golay, X. (2007). Optimized MRI Parameters for Positive Contrast Detection of Iron-oxide Labeled Cells Using Double-echo Ultra-short Echo Time (d-UTE) Sequences, *Proceedings of Intl Soc Magn Reson Med*, ISSN 1545-4436/2005, Berlin, Germany, May 2007
- Crowe, L., Wang, Y., Gatehouse P., Tessier, J., Waterton, J., Robert, P., Bydder, G., & Firmin, D. (2005). Ex vivo MR Imaging of Atherosclerotic Rabbit Aorta Labelled with USPIO – Enhancement of Iron Loaded Regions in UTE Imaging, *Proceedings of Intl Soc Magn Reson Med*, ISSN 1545-4436, Miami Beach, Florida, USA, May 2005
- Cunningham, C., Arai, T., Yang, P., McConnell, M., Pauly, J., & Conolly, S. (2005). Positive Contrast Magnetic Resonance Imaging of Cells Labeled with Magnetic Nanoparticles. *Magn Reson Med*, Vol. 53, No. 5, (April 2005), pp. 999–1005, ISSN 0740-3194
- Dahnke, H., Liu, W., Herzka, D., Frank, J., & Schaeffter, T. (2008). Susceptibility Gradient Mapping (SGM): A New Postprocessing Method for Positive Contrast Generation Applied to Superparamagnetic Iron Oxide Particle (SPIO)-labeled Cells. *Magn Reson Med*, Vol. 60, No. 3, (August 2008), pp. 595–603, ISSN 0740-3194
- de Vries, I., Lesterhuis, W., Barentsz, J., Verdijk, P., van Krieken, J., Boerman, O., Oyen, W., Bonenkamp, J., Boezeman, J., Adema, G., Bulte, J., Scheenen, T., Punt, C., Heerschap, A., & Figdor, C. (2005). Magnetic Resonance Tracking of Dendritic Cells in Melanoma Patients for Monitoring of Cellular Therapy. *Nature Biotechnology*, Vol. 23, No. 11, (October 2005), pp. 1407–1413, ISSN 1087-0156
- Dharmakumar, R., Koktzoglou, I., & Li, D. (2006). Generating Positive Contrast from Off-Resonant Spins with Steady-state Free Precession Magnetic Resonance Imaging: Theory and Proof-of-principle Experiments. *Phys. Med. Biol.*, Vol. 51, No. 17, (August 2006), pp. 4201-4215, ISSN 0031-9155
- Dharmakumar, R., Koktzoglou, I., & Li, D. (2007). Factors Influencing Fast Low Angle Positive Contrast Steady-state Free Precession (FLAPS) Magnetic Resonance Imaging. *Phys. Med. Biol.*, Vol. 52, No. 11, (May 2007), pp. 3261-3273, ISSN 0031-9155
- Dharmakumar, R., Zhang, Z., Koktzoglou, I., Tsaftaris, S., & Li, D. (2009). Dual-contrast Cellular Magnetic Resonance Imaging. *Mol Imaging*, Vol. 8, No. 5, (October 2009), pp. 254-263, ISSN 1535-3508
- Dixon, W., Blezek, D., Lowery, L., Meyer, D., Kulkarni, A., Bales, B., Petko, D., Foo, T. (2009). Estimating Amounts of Iron Oxide from Gradient Echo Images. *Magn Reson Med*, Vol. 61, No. 5, (February 2009), pp. 1132–1136, ISSN 0740-3194
- Farrar, C., Dai, G., Novikov, M., Rosenzweig, A., Weissleder, R., Rosen, B., Sosnovik, D. (2008). Impact of Field Strength and Iron Oxide Nanoparticle Concentration on The Linearity and Diagnostic Accuracy of Off-resonance Imaging. *NMR Biomed*, Vol. 21, No. 5, (October 2007), pp. 453-463, ISSN 0952-3480

- Ferrucci, J., & Stark, D. (1990). Iron Oxide-enhanced MR Imaging of The Liver and Spleen: Review of the First 5 years. *AJR Am J Roentgenol*, Vol. 155, No. 5, (November 1990), pp. 943-950, ISSN 0361-803X
- Foltz, W., Cunningham, C., Mutsaers, A., Conolly, S., Stewart, D., & Dick, A. (2006). Positive-contrast Imaging in the Rabbit Hind-limb of Transplanted Cells Bearing Endocytosed Superparamagnetic Beads. *J Cardiovasc Magn Reson*, Vol. 8, No. 6, (November 2006), pp. 817-823, ISSN 1097-6647
- Frank, J., Anderson, S., Kalsih, H., Jordan, E., Lewis, B., Yocum, G., & Arbab, A. (2004). Methods For Magnetically Labeling Stem and Other Cells for Detection by In Vivo Magnetic Resonance Imaging. *Cytotherapy*, Vol. 6, No. 6, (November 2004), pp. 621-625, ISSN 1465-3249
- Genove, G., DeMarco, U., Xu, H., Goins, W., & Ahrens, E. (2005). A New Transgene Reporter for In Vivo Magnetic Resonance Imaging. *Nat Med*, Vol. 11, No. 4, (April 2005), pp. 450-454, ISSN 1078-8956
- Girard, O., Du, J., Agemy, L., Sugahara, K., Kotamraju, V., Ruoslahti, E., Bydder, G., & Mattrey, R. (2011). Optimization of Iron Oxide Nanoparticle Detection Using Ultrashort Echo Time Pulse Sequences: Comparison of T1, T2*, and Synergistic T1 – T2* Contrast Mechanisms. *Magn Reson Med*, Vol. 65, No. 6, (February 2011), pp. 1649-1660, ISSN 0740-3194
- Gonzalez-Lara, L., Xu, X., Hofstetrova, K., Pniak, A., Brown, A., & Foster, P. (2009). In Vivo Magnetic Resonance Imaging of Spinal Cord Injury in The Mouse. *J Neurotrauma*, Vol. 26, No. 5, (May 2009), pp. 753-762, ISSN 0897-7151
- Grodzki, D., Jakob, P., & Heismann, B. (2011). Ultrashort Echo Time Imaging Using Pointwise Encoding Time Reduction with Radial Acquisition (PETRA). *Magn Reson Med*, Article first published online : 30 JUN 2011, ISSN 0740-3194
- Gupta, T., Virmani, S., Neidt, T., Szolc-Kowalska, B., Sato, K., Ryu, R., Lewandowski, R., Gates, V., Woloschak, G., Salem, R., Omary, R., & Larson, A. (2008). MR Tracking of Iron-labeled Glass Radioembolization Microspheres during Transcatheter Delivery to Rabbit VX2 Liver Tumors: Feasibility Study. *Radiology*, Vol. 249, No. 3, (October 2008), pp. 845-854, ISSN 0033-8419
- Guthi, J., Yang, S., Huang, G., Li, S., Khemtong, C., Kessinger, C., Peyton, M., Minna, J., Brown, K., & Gao, J. (2010). MRI-visible Micellar Nanomedicine for Targeted Drug Delivery to lung cancer cells. *Mol Pharm*, Vol. 7, No. 1, (February 2010), pp. 32-40, ISSN 1543-8384
- Helmberger, T., & Semelka, R. (2001). New Contrast Agents for Imaging The Liver. *Magn Reson Imaging Clin N Am*, Vol. 9, No. 4, (November 2001), pp. 745-766, ISSN 1064-9689
- Herschman, H. (2003). Molecular Imaging: Looking At Problems, Seeing Solutions. *Science*, Vol. 302, No. 5645, (October 2003), pp. 605-608, ISSN 0036-8075
- Heyn, C., Bowen, C., Rutt, B., & Foster, P. (2005). Detection Threshold of Single SPIO-labeled Cells with FIESTA. *Magn Reson Med*, Vol. 53, No. 2, (February 2005), pp. 312-320, ISSN 0740-3194
- Heyn, C., Ronald, J., Mackenzie, L., MacDonald, I., Chambers, A., Rutt, B., Foster, P. (2006). In Vivo Magnetic Resonance Imaging of Single Cells in Mouse Brain with Optical Validation. *Magn Reson Med*, Vol. 55, No. 1, (January 2006), pp. 23-29, ISSN 0740-3194

- Högemann-Savellano, D., Bos, E., Blondet, C., Sato, F., Abe, T., Josephson, L., Weissleder, R., Gaudet, J., Sgroi, D., Peters, P., & Basilion, J. (2003). The Transferrin Receptor: a Potential Molecular Imaging Marker for Human Cancer. *Neoplasia*, Vol. 5, No. 6, (November 2003), pp. 495- 506, ISSN 1522-8002
- Hsiao, J., Tai, M., Chu, H., Chen, S., Li, H., Lai, D., Hsieh, S., Wang, J., & Liu, H. (2007). Magnetic Nanoparticle Labeling of Mesenchymal Stem Cells Without Transfection Agent: Cellular Behavior and Capability of Detection with Clinical 1.5T Magnetic Resonance at The Single Cell Level. *Magn Reson Med*, Vol. 58, No. 4, (October 2006), pp. 717-724, ISSN 0740-3194
- Jaffer, F., Libby, P., & Weissleder, R. (2009). Optical and Multimodality Molecular Imaging: Insights Into Atherosclerosis. *Arterioscler Thromb Vasc Biol.*, Vol. 29, No. 7, (July 2009), pp. 1017-1024. ISSN 1079-5642
- Kelloff, G., Krohn, K., Larson, S., Weissleder, R., Mankoff, D., Hoffman, J., Link, J., Guyton, K., Eckelman, W., Scher, H., O'Shaughnessy, J., Cheson, B., Sigman, C., Tatum, J., Mills, G., Sullivan, D., & Woodcock, J. (2005). The Progress and Promise of Molecular Imaging Probes in Oncologic Drug Development. *Clin Cancer Research*, Vol. 11, No. 22, (November 2005), pp. 7967-7985, ISSN 1078-0432
- Khakoo, A., Pati, S., Anderson, S., Reid, W., Elshal, M., Rovira, I., Nguyen, A., Malide, D., Combs, C., Hall, G., Zhang, J., Raffeld, M., Rogers, T., Stetler-Stevenson, W., Frank, J., Reitz, M., & Finkel, T. (2006). Human Mesenchymal Stem Cells Exert Potent Antitumorigenic Effects in A Model of Kaposi's Sarcoma. *J Exp Med*, Vol. 203, No. 5, pp. 1235-1247, ISSN 0022-1007
- Khemtong, C., Kessinger, C., Ren, J., Bey, E., Yang, S., Guthi, J., Boothman, D., Sherry, A., & Gao, J. (2009). In Vivo Off-resonance Saturation Magnetic Resonance Imaging of Alphasbeta3-targeted Superparamagnetic Nanoparticles. *Cancer Res*, Vol. 69, No. 4, (February 2009), pp. 1651-1658, ISSN 0008-5472
- Kim, Y., Bae, K., Lee, Y., Park, T., Yoo, S., & Park, H. (2006). Positive-Contrast Cellular MR Imaging Using Susceptibility Weighted Echo-time Encoding Technique (SWEET), *World Congress on Medical Physics and Biomedical Engineering*, ISBN 9783540368397, Coex Seoul, Korea, August 2006
- Kim, Y., Bae, K., Yoo, S., Park, T., & Park, H. (2009). Positive Contrast Visualization for Cellular Magnetic Resonance Imaging Using Susceptibility-weighted Echo-time Encoding. *Magn Reson Imaging*, Vol. 27, No. 5, (December 2008), pp. 601-610, 0730-725X
- Kircher, M., Allport, J., Graves, E., Love, V., Josephson, L., Lichtman, A., & Weissleder, R. (2003a). In Vivo High Resolution Three-dimensional Imaging of Antigen-specific Cytotoxic T-lymphocyte Trafficking to Tumors. *Cancer Res*, Vol. 63, No. 20, (October 2003), pp. 6838-6846, ISSN 0008-5472
- Kircher, M., Mahmood, U., King, R., Weissleder, R., & Josephson, L. (2003b). A Multimodal Nanoparticle for Preoperative Magnetic Resonance Imaging and Intraoperative Optical Brain Tumor Delineation. *Cancer Res*, Vol. 63, No. 23, (December 2003), pp. 8122-8125, ISSN 0008-5472
- Korosoglou, G., Shah, S., Vonken, E., Gilson, W., Schär, M., Tang, L., Kraitchman, D., Boston, R., Sosnovik, D., Weiss, R., Weissleder, R., & Stuber, M. (2008a). Off Resonance Angiography: A New Method to Depict Vessels—phantom and Rabbit Studies. *Radiology*, Vol. 249, No. 2, (September 2008), pp. 501-509, ISSN 0033-8419

- Korosoglou, G., Weiss, R., Kedziorek, D., Walczak, P., Gilson, W., Schär, M., Tang, L., Kraitchman, D., Boston, R., Sosnovik, D., Weiss, R., Bulte, J., Weissleder, R., & Stuber, M. (2008b). Noninvasive Detection of Macrophage-rich Atherosclerotic Plaque in Hyperlipidemic Rabbits Using "Positive contrast" Magnetic Resonance Imaging. *J Am Coll Cardiol*, Vol. 52, No. 6, (August 2008), pp. 483-491, ISSN 0735-1097
- Korosoglou, G., Tang, L., Kedziorek, D., Cosby, K., Gilson, W., Vonken, E., Schär, M., Sosnovik, D., Kraitchman, D., Weiss, R., Weissleder, R., & Stuber, M. (2008c). Positive Contrast MR-lymphography Using Inversion Recovery with ON-resonant Water Suppression (IRON). *J Magn Reson Imaging*, Vol. 27, No. 5, (May 2008), pp. 1175-1180, ISSN 1053-1807
- Kraitchman, D., Tatsumi, M., Gilson, W., Ishimori, T., Kedziorek, D., Walczak, P., Segars, W., Chen, H., Fritzges, D., Izbudak, I., Young, R., Marcelino, M., Pittenger, M., Solaiyappan, M., Boston, R., Tsui, B., Wahl, R., & Bulte, J. (2005). Dynamic Imaging of Allogeneic Mesenchymal Stem Cells Trafficking to Myocardial Infarction. *Circulation*, Vol. 112, No. 10, (August 2005), pp. 1451-1461. ISSN 0009-7322
- Kuhlpeter, R., Dahnke, H., Matuszewski, L., Persigehl, T., von Wallbrunn, A., Allkemper, T., Heindel, W., Schaeffter, T., & Bremer, C. (2007). R2 and R2 Mapping for Sensing Cell-Bound Superparamagnetic Nanoparticles. *Radiology*, Vol. 245, No. 2, (September 2007), pp. 449-457, ISSN 0033-8419
- Langley, J., Liu, W., Jordan, E., Frank, J., & Zhao, Q. (2011). Quantification of SPIO Nanoparticles In Vivo Using the Finite Perturber Method. *Magn Reson Med*, Vol. 65, No. 5, (November 2010), pp. 1461-1469, ISSN 0740-3194
- Lee, H., Li, Z., Chen, K., Hsu, A., Xu, C., Xie, J., Sun, S., & Chen, X. (2008). PET/MRI Dual-Modality Tumor Imaging Using Arginine-glycine-aspartic (RGD)-conjugated Radiolabeled Iron Oxide Nanoparticles. *J Nucl Med*, Vol. 49, No. 8, (July 2008), 1371-1379. ISSN 0161-5505
- Lefevre S, Ruimy D, Jehl F, Neuville A, Robert P, Sordet C, Ehlinger M, Dietemann JL, Bierry G. (2011). Septic Arthritis: Monitoring with USPIO-enhanced Macrophage MR Imaging. *Radiology*, Vol. 258, No. 3, (March 2011), pp. 722-728, ISSN 0033-8419
- Li, W., Tutton, S., Vu, A., Pierchala, L., Li, B., Lewis, J., Prasad, P., & Edelman, R. (2005). First-pass Contrast-enhanced Magnetic Resonance Angiography in Humans Using Ferumoxytol, A Novel Ultrasmall Superparamagnetic Iron Oxide (USPIO)-based Blood Pool Agent. *J Magn Reson Imaging*, Vol. 1, No. 5, (January 2005), pp. 46-52, ISSN 1053-1807
- Liu, C., Ren, J., Yang, J., Liu, C., Mandeville, J., Rosen, B., Bhide, P., Yanagawa, Y., & Liu, P. (2009). Dna-based Mri Probes for Specic Detection of Chronic Exposure to Amphetamine in Living Brains. *The Journal of Neuroscience*, Vol. 29, No. 34, (August 2009), pp. 10663-10670, ISSN 0270-6474
- Liu, H., Hua, M., Yang, H., Huang, C., Chu, P., Wu, J., Tseng, I., Wang, J., Yen, T., Chen, P., & Wei, K. (2010). Magnetic Resonance Monitoring of Focused Ultrasound/Magnetic Nanoparticle Targeting Delivery of Therapeutic Agents to the Brain. *Proc Natl Acad Sci U S A.*, Vol. 107, No. 34, (August 2010), pp. 15205-15210, ISSN 0027-8424
- Liu, W., Dahnke, H., Jordan, E., Schaeffter, T., & Frank, J. (2008). In Vivo MRI Using Positive-contrast Techniques in Detection of Cells Labeled with Superparamagnetic

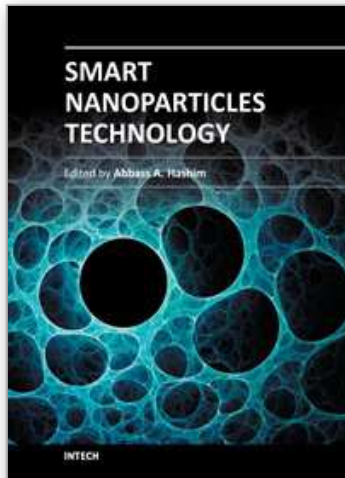
- Iron Oxide Nanoparticles. *NMR Biomed*, Vol. 21, No. 3, (March 2008), pp. 242-250, ISSN 0952-3480
- Liu, W., Dahnke, H., Rahmer, J., Jordan, E., & Frank, J. (2009). Ultrashort T2* Relaxometry for Quantitation of Highly Concentrated Superparamagnetic Iron Oxide (SPIO) Nanoparticle Labeled Cells. *Magn Reson Med*, Vol. 61, No. 4, (April 2009), pp. 761-766, ISSN 0740-3194
- Mani, V., Briley-Saebo, K., Hyafil, F., & Fayad, Z. (2006a). Feasibility of In Vivo Identification of Edogenous Ferritin with Positive Contrast MRI in Rabbit Carotid Crush Injury Using GRASP. *Magn Reson Med*, Vol. 56, No. 5, (November 2006), pp. 1096-1106, ISSN 0740-3194
- Mani, V., Briley-Saebo, K., Itskovich, V., Samber, D., & Fayad, Z. (2006b). Gradient Echo Acquisition for Superparamagnetic Particles with Positive Contrast (GRASP): Sequence Characterization in Membrane and Glass Superparamagnetic Iron Oxide Phantoms at 1.5 T and 3 T. *Magn Reson Med*, Vol. 55, No. 1, (January 2006), pp. 126-135, ISSN 0740-3194
- Mani, V., Adler, E., Briley-Saebo, K., Bystrup, A., Fuster, V., Keller, G., & Fayad, Z. (2008). Serial In Vivo Positive Contrast MRI of Iron Oxide-labeled Embryonic Stem Cell Derived Cardiac Precursor Cells in A Mouse Model of Myocardial Infarction. *Magn Reson Med*, Vol. 60, No. 1, (July 2008), pp. 73-81, ISSN 0740-3194
- Manninger, S., Muldoon, L., Nesbit, G., Murillo, T., Jacobs, P., & Neuwelt, E. (2005). An Exploratory Study of Ferumoxtran-10 Nanoparticles as a Blood-brain barrier Imaging Agent Targeting Phagocytic Cells in CNS Inflammatory Lesions. *AJNR Am J Neuroradiol.*, Vol. 26, No. 9, (October 2005), pp. 2290-2300.
- Medarova, Z., Pham, W., Farrar, C., Petkova, V., & Moore, A. (2007). In Vivo Imaging of siRNA Delivery and Silencing in Tumors. *Nat Med*, Vol. 13, No. 3, (February 2007), pp. 372-377, ISSN 1078-8956
- Metz, S., Beer, A., Settles, M., Pelisek, J., Botnar, R., Rummeny, E., & Heider, P. (2011). Characterization of Carotid Artery Plaques with USPIO-enhanced MRI: Assessment of Inflammation and Vascularity as In Vivo Imaging Biomarkers for Plaque Vulnerability. *Int J Cardiovasc Imaging*, Vol. 27, No. 6, (October 2010), pp. 901-912, ISSN 1569-5794
- Modo, M., Hoehn, M., & Bulte, J. (2005). Cellular MR imaging. *Mol Imaging.*, Vol. 4, No. 3, (July 2005), pp. 143-164, ISSN 1535-3508
- Muja, N., & Bulte, J. (2009). Magnetic Resonance Imaging of Cells in Experimental Disease Models. *Prog Nucl Magn Reson Spectrosc.*, Vol. 55, No. 1, (July 2009), pp. 61-77, ISSN 0079-6565
- Nasongkla, N., Bey, E., Ren, J., Ai, H., Khemtong, C., Guthi, J., Chin, S., Sherry, A., Boothman, D., & Gao, J. (2006). Multifunctional Polymeric Micelles as Cancer-targeted, MRI-ultrasensitive Drug Delivery Systems. *Nano Lett.*, Vol. 6, No. 11, (November 2006), pp. 2427-2430, ISSN 1530-6984
- Niu, G., & Chen, X. (2011). Why Integrin as A Primary Target for Imaging and Therapy. *Theranostics*, Vol. 1, No. 1, (January 2011), pp. 30-47, ISSN 1838-7640
- Oude Engberink, R., van der Pol, S., Döpp, E., de Vries, H., & Blezer, E. (2007). Comparison of SPIO and USPIO for In Vitro Labeling of Human Monocytes: MR Detection and Cell Function. *Radiology*, Vol. 243, No. 2, (May 2007), pp. 467-474, ISSN 0033-8419

- Politi, L., Bacigaluppi, M., Brambilla, E., Cadioli, M., Falini, A., Comi, G., Scotti, G., Martino, G., & Pluchino, S. (2007). Magnetic-resonancebased Tracking and Quantification of Intravenously Injected Neural Stem Cell Accumulation in The Brains of Mice with Experimental Multiple Sclerosis. *Stem Cells*, Vol. 25, No. 10, (Jun 2007), pp. 2583-2592, ISSN 0250-6793
- Rad, A., Arbab, A., Iskander, A., Jiang, Q., & Soltanian-Zadeh, H. (2007). Quantification of Superparamagnetic Iron Oxide (SPIO)-labeled Cells Using MRI. *J Magn Reson Imaging*, Vol. 26, No. 2, (August 2007), pp 366-374, ISSN 1053-1807
- Rahmer, J., Bornert, P., & Dries, S. Assessment of Anterior Cruciate Ligament Reconstruction Using 3D Ultrashort Echo-time MR Imaging. (2009). *J Magn Reson Imaging*, Vol. 29, No. 2, (February 2009), pp 443-448, ISSN 1053-1807
- Reimer, P., Rummeny, E., Daldrup, H., Balzer, T., Tombach, B., Berns, T., & Peters, P. (1995). Clinical Results with Resovist: A Phase 2 Clinical Trial. *Radiology*, Vol. 195, No. 2, (May 1995), pp. 489-496, ISSN 0033-8419
- Righi, V., Andronesi, O., Mintzopoulos, D., Fichman, A., & Tzika, A. (2010). Molecular MR Imaging of Labeled Stem Cells in A Mouse Burn Model In Vivo, *Proceedings of Intl Soc Magn Reson Med*, ISSN 1545-4436, Stockholm, Sweden, May 2010
- Robson, M., & Bydder, G. (2006). Clinical Ultrashort Echo Time Imaging of Bone and Other Connective Tissues. *NMR Biomed*, Vol. 19, No. 7, (November 2006), pp. 765-780, ISSN 0952-3480
- Seevinck, P., de Leeuw, H., Bos, C., & Bakker, C. (2011). Highly Localized Positive Contrast of Small Paramagnetic Objects Using 3D Center-out Radial Sampling with Off-resonance Reception. *Magn Reson Med*, Vol. 65, No. 1, (January 2008), pp. 146-156, ISSN 0740-3194
- Seppenwoolde, J., Viergever, M., & Bakker, C. (2003). Passive Tracking Exploiting Local Signal Conservation: The White Marker Phenomenon. *Magn Reson Med*, Vol. 50, No. 4, (October 2003), pp. 784-790, ISSN 0740-3194
- Seppenwoolde, J., Vincken, K., & Bakker, C. (2007). White-marker Imaging-Separating Magnetic Susceptibility Effects from Partial Volume Effects. *Magn Reson Med*, Vol. 58, No. 3, (September 2007), pp. 605-609, ISSN 0740-3194
- Shapiro, E., Skrtic, S., & Koretsky, A. (2005). Sizing It Up: Cellular Mri Using Micron-sized Iron Oxide Particles. *Magn Reson Med*, Vol. 53, No. 2, (February 2005), pp. 329-338, ISSN 0740-3194
- Sigovan, M., Hamoudeh, M., Al Faraj, A., Charpigny, D., Fessi, H., & Canet-Soulas, E. (2011). Positive Contrast with Therapeutic Iron Nanoparticles at 4.7 T. *MAGMA*, Vol. 24, No. 5, (May 2011), pp. 259-265, ISSN 0968-5243
- Small, W., Nelson, R., & Bernardino, M. (1993). Dual-contrast Enhancement of Both T1- and T2-weighted Sequences Using Ultra Small Superparamagnetic Iron Oxide. *Magn Reson Med*, Vol. 11, No. 5, (May 1993), pp. 645-654, ISSN 0740-3194
- Sosnovik, D. (2009). Molecular Imaging of Myocardial Injury: A Magnetofluorescent Approach. *Curr Cardiovasc Imaging Rep.*, Vol. 2, No. 1, (February 2009), pp. 33-39, ISSN 1941-9066
- Stuber, M., Gilson, W., Schaer, M., Bulte, J., & Kraitchman, D. (2005). Shedding Light on the Dark Spot with IRON - A Method That Generates Positive Contrast in The Presence of Superparamagnetic Nanoparticles, *Proceedings of Intl Soc Magn Reson Med*, ISSN 1545-4436, Miami Beach, Florida, USA, May 2005

- Stuber, M., Gilson, W., Schär, M., Kedziorek, D., Hofmann, L., Shah, S., Vonken, E., Bulte, J., & Kraitchman, D. (2007). Positive Contrast Visualization of Iron Oxide-labeled Stem Cells Using Inversion-recovery with ON-resonant Water Suppression (IRON). *Magn Reson Med*, Vol. 58, No. 5, (November 2007), pp. 1072-1077, ISSN 0740-3194
- Suzuki, Y., Cunningham, C., Noguchi, K., Chen, I., Weissman, I., Yeung, A., Robbins, R., & Yang, P. (2008). In Vivo Serial Evaluation of Superparamagnetic Iron-oxide Labeled Stem Cells by Off-resonance Positive Contrast. *Magn Reson Med*, Vol. 60, No. 6, (December 2008), pp. 1269-1275, ISSN 0740-3194
- Tan, M., & Lu, Z. (2011). Integrin Targeted MR Imaging. *Theranostics*, Vol. 1, No. 1, (January 2011), pp. 30-47, ISSN 1838-7640.
- Tang, Y., Yamashita, Y., Arakawa, A., Namimoto, T., Mitsuzaki, K., Abe, Y., Katahira, K., & Takahashi, M. (1999). Detection of Hepatocellular Carcinoma Arising in Cirrhotic Livers: Comparison of Gadolinium- and Ferumoxides Enhanced MR Imaging. *AJR Am J Roentgenol*, Vol. 172, No. 6, pp. 1547-1554, ISSN 0361-803X
- Thorek, D., Chen, A., Czupryna, J., & Tsourkas, A. (2006). Superparamagnetic Iron Oxide Nanoparticle Probes for Molecular Imaging. *Ann Biomed Eng*, Vol. 34, No. 1, (January 2006), pp. 23-38, ISSN 0090-6964
- Trivedi, R., Mallawarachi, C., U-King-Im, J., Graves, M., Horsley, J., Goddard, M., Brown, A., Wang, L., Kirkpatrick, P., Brown, J., & Gillard, J. (2006). Identifying Inflamed Carotid Plaques Using In Vivo USPIO-enhanced MR Imaging to Label Plaque Macrophages. *Arterioscler Thromb Vasc Biol*, Vol. 26, No. 7, (July 2006), pp. 1601-1606, ISSN 1079-5642
- Weiseh, O., Gunn, J., & Zhang, M. (2010). Design and Fabrication of Magnetic Nanoparticles for Targeted Drug Delivery and Imaging. *Adv Drug Deliv Rev*, Vol. 62, No. 3, (November 2009), pp. 284-304, ISSN 0169-409X
- Ward, K., Aletras, A., & Balaban, R. (2000). A New Class of Contrast Agents for MRI Based on Proton Chemical Exchange Dependent Saturation Transfer (CEST). *J Magn Reson.*, Vol. 143, No. 1, (March 2000), pp. 79-87, ISSN 1090-7807
- Weissleder, R., Elizondo, G., Wittenberg, J., Rabito, C., Bengel, H., & Josephson, L. (1990). Ultrasmall Superparamagnetic Iron Oxide: Characterization of a New Class of Contrast Agents for MR Imaging. *Radiology*, Vol. 175, No. 2, (May 1990), pp. 489-493, ISSN 0033-8419
- Xie, J., Chen, K., Huang, J., Lee, S., Wang, J., Gao, J., Li, X., & Chen, X. (2010). PET/NIRF/MRI Triple Functional Iron Oxide Nanoparticles. *Biomaterials*, Vol. 31, No. 11, (April 2010), pp. 3016-3022, ISSN 0142-9612
- Yamamoto, H., Yamashita, Y., Yoshimatsu, S., Baba, Y., Hatanaka, Y., Murakami, R., Nishiharu, T., Takahashi, M., Higashida, Y., & Moribe, N. (1995). Hepatocellular Carcinoma in Cirrhotic Livers: Detection with Unenhanced and Iron Oxide-enhanced MR Imaging. *Radiology*, Vol. 195, No. 1, (April 1995), pp. 106-112, ISSN 0033-8419
- Yang, H., Zhuang, Y., Sun, Y., Dai, A., Shi, X., Wu, D., Li, F., Hu, H., & Yang, S. Targeted Dual-contrast T(1)- and T(2)-weighted Magnetic Resonance Imaging of Tumors Using Multifunctional Gadolinium-labeled Superparamagnetic Iron Oxide Nanoparticles. *Biomaterials*, Vol. 32, No. 20, (March 2011), pp. 4584-4593, ISSN 0142-9612

- Zhang, L., Zhong, X., Wang, L., Chen, H., Wang, Y., Yeh, J., Yang, L., & Mao, H. T1-weighted Ultrashort Echo Time Method for Positive Contrast Imaging of Magnetic Nanoparticles and Cancer Cells bound with the Targeted Nanoparticles. *J Magn Reson Imaging*, Vol. 33, No. 1, (January 2011), pp. 194-202, ISSN 1053-1807
- Zhang, Z., Dharmakumar, R., Mascheri, N., Fan, Z., Wu, S., & Li, D. (2009). Comparison of SPIO and USPIO Cell Labeling for Tracking GFP Gene Marker with Negative and Positive Contrast MRI. *Mol Imaging*, Vol. 8, No. 3, (October 2009), pp. 148-155, ISSN 1535-3508
- Zhang, Z., Mascheri, N., Dharmakumar, R., & Li, D. (2008). Cellular Magnetic Resonance Imaging: Potential for Use in Assessing Aspects of Cardiovascular Disease. *Cytotherapy*, Vol. 10, No. 6, (March 2008), pp. 575-586, ISSN 1465-3249
- Zhang, Z., van den Bos, E., Wielopolski, P., de Jong-Popijus, M., Bernsen, M., Duncker, D., & Krestin, G. (2005). In Vitro Imaging of Single Living Human Umbilical Vein Endothelial Cells with a Clinical 3.0-T MRI Scanner. *MAGMA*, Vol. 18, No. 4, (August 2005), pp. 175-185, ISSN 0968-5243
- Zhao, M., Kircher, M., Josephson, L., & Weissleder, R. (2002). Differential Conjugation of Tat Peptide to Superparamagnetic Nanoparticles and Its Effect on Cellular Uptake. *Bioconjug Chem*, Vol. 13, No. 4, (July 2002), pp. 840-844.
- Zhao, Q., Langley, J., Lee, S., & Liu, W. (2011). Positive Contrast Technique for the Detection and Quantification of Superparamagnetic Iron Oxide Nanoparticles in MRI. *NMR Biomed*, Vol. 24, No. 5, (October 2010), pp. 464-472, ISSN 0952-3480
- Zhu, J., Zhou, L., & XingWu, F. (2006). Tracking Neural Stem Cells in Patients with Brain Trauma. *N Engl J Med.*, Vol. 30, No. 355, (November 2006), pp. 2376-2378, ISSN 0028-4793
- Zurkiya, O., Chan, A., & Hu, X. (2008). MagA is Sufficient for Producing Magnetic Nanoparticles in Mammalian Cells, Making It an MRI Reporter. *Magn Reson Med*, Vol. 59, No. 6, (Jun 2008), pp. 1225-1231, ISSN 0740-3194
- Zurkiya, O., & Hu, X. (2006). Off-resonance Saturation as a Means of Generating Contrast with Superparamagnetic Nanoparticles. *Magn Reson Med*, Vol. 56, No. 4, (October 2006), pp. 726-732, ISSN 0740-3194

IntechOpen



Smart Nanoparticles Technology

Edited by Dr. Abbass Hashim

ISBN 978-953-51-0500-8

Hard cover, 576 pages

Publisher InTech

Published online 18, April, 2012

Published in print edition April, 2012

In the last few years, Nanoparticles and their applications dramatically diverted science in the direction of brand new philosophy. The properties of many conventional materials changed when formed from nanoparticles. Nanoparticles have a greater surface area per weight than larger particles which causes them to be more reactive and effective than other molecules. In this book, we (InTech publisher, editor and authors) have invested a lot of effort to include 25 most advanced technology chapters. The book is organised into three well-heelled parts. We would like to invite all Nanotechnology scientists to read and share the knowledge and contents of this book.

How to reference

In order to correctly reference this scholarly work, feel free to copy and paste the following:

Shengyong Wu (2012). Iron Oxide Nanoparticles Imaging Tracking by MR Advanced Techniques: Dual-Contrast Approaches, Smart Nanoparticles Technology, Dr. Abbass Hashim (Ed.), ISBN: 978-953-51-0500-8, InTech, Available from: <http://www.intechopen.com/books/smart-nanoparticles-technology/iron-oxide-nanoparticles-imaging-tracking-by-mr-advanced-techniques-dual-contrast-approaches>

INTECH
open science | open minds

InTech Europe

University Campus STeP Ri
Slavka Krautzeka 83/A
51000 Rijeka, Croatia
Phone: +385 (51) 770 447
Fax: +385 (51) 686 166
www.intechopen.com

InTech China

Unit 405, Office Block, Hotel Equatorial Shanghai
No.65, Yan An Road (West), Shanghai, 200040, China
中国上海市延安西路65号上海国际贵都大饭店办公楼405单元
Phone: +86-21-62489820
Fax: +86-21-62489821

© 2012 The Author(s). Licensee IntechOpen. This is an open access article distributed under the terms of the [Creative Commons Attribution 3.0 License](#), which permits unrestricted use, distribution, and reproduction in any medium, provided the original work is properly cited.

IntechOpen

IntechOpen